

More Benefits of Semileptonic Rare B Decays at Low Recoil: CP Violation

Christoph Bobeth

*Institute for Advanced Study & Excellence Cluster Universe,
Technische Universität München, D-85748 Garching, Germany*

Gudrun Hiller and Danny van Dyk

Institut für Physik, Technische Universität Dortmund, D-44221 Dortmund, Germany

Abstract

We present a systematic analysis of the angular distribution of $\bar{B} \rightarrow \bar{K}^*(\rightarrow \bar{K}\pi)l^+l^-$ decays with $l = e, \mu$ in the low recoil region (i.e. at high dilepton invariant masses of the order of the mass of the b -quark) to account model-independently for CP violation beyond the Standard Model, working to next-to-leading order QCD. From the employed heavy quark effective theory framework we identify the key CP observables with reduced hadronic uncertainties. Since some of the CP asymmetries are CP-odd they can be measured without B -flavour tagging. This is particularly beneficial for $\bar{B}_s, B_s \rightarrow \phi(\rightarrow K^+K^-)l^+l^-$ decays, which are not self-tagging, and we work out the corresponding time-integrated CP asymmetries. Presently available experimental constraints allow the proposed CP asymmetries to be sizeable, up to values of the order ~ 0.2 , while the corresponding Standard Model values receive a strong parametric suppression at the level of $\mathcal{O}(10^{-4})$. Furthermore, we work out the allowed ranges of the short-distance (Wilson) coefficients $\mathcal{C}_{9,10}$ in the presence of CP violation beyond the Standard Model but no further Dirac structures. We find the $\bar{B}_s \rightarrow \mu^+\mu^-$ branching ratio to be below 9×10^{-9} (at 95% CL). Possibilities to check the performance of the theoretical low recoil framework are pointed out.

I. INTRODUCTION

The exclusive rare flavour changing neutral current (FCNC) decay $\bar{B} \rightarrow \bar{K}^*(\rightarrow \bar{K}\pi)l^+l^-$ with $l = e, \mu$ has high sensitivity to physics beyond the Standard Model (BSM) due to the large number of complementary measurements possible from the full angular distribution [1]. Many works have focussed on the region of low dilepton invariant mass squared, q^2 , typically taken within the range 1–6 GeV². The latter is accessible to QCD factorisation [2, 3], which has enabled systematic studies of CP-averaged observables as well as CP-asymmetries [4–8]. Intermediate values of q^2 fall into the narrow-resonance region dominated by the pronounced $c\bar{c}$ -resonance background from the decays $\bar{B} \rightarrow \bar{K}^* \{J/\psi, \psi'\} \rightarrow \bar{K}^*l^+l^-$, recently studied in [9] including also low q^2 tails. At larger dilepton masses, at about $q^2 \gtrsim 14$ GeV², follows the broad resonance region. The latter is characterised by the low recoil of the hadronic system. Here, the large values of $q^2 \sim m_b^2$, where m_b denotes the mass of the b -quark, allow to perform an operator product expansion (OPE) [10, 11] which, when combined with heavy quark effective theory (HQET) and the corresponding heavy quark form factor relations [12], leads to powerful predictions, see [10] and Hurth and Wyler in [13]. In fact, it has been shown recently that the heavy quark framework applied to the low recoil region results in a very simple amplitude structure of the decays $\bar{B} \rightarrow \bar{K}^*(\rightarrow \bar{K}\pi)l^+l^-$ [14]. Specifically, in the heavy quark limit, all three participating transversity amplitudes obey

$$A_i^{L,R} \propto C^{L,R} \times f_i, \quad i = \perp, \parallel, 0, \quad (1.1)$$

hence factorise into universal short-distance coefficients $C^{L,R}$ and form factor coefficients f_i . This feature can be greatly exploited to enhance the BSM sensitivity, to test form factor predictions against data and to check the goodness of the OPE framework. More explicit, the angular distribution of $\bar{B} \rightarrow \bar{K}^*(\rightarrow \bar{K}\pi)l^+l^-$ decays allows for observables with the following salient properties, see [14] for details:

- i*) The observable $H_T^{(1)} = 1$ does *not* depend on short-distance coefficients *nor* on form factors.
- ii*) The observables $H_T^{(2,3)}$ depend on the short-distance coefficients only, and obey $H_T^{(2)} = H_T^{(3)}$.
- iii*) Several observables can be formed which depend on the form factors only.
- iv*) The angular observables $J_{7,8,9}$, which are odd under naive time-reversal, vanish.

Beyond zeroth order in $1/m_b$, the influence of the power corrections is weak because the Λ_{QCD}/m_b corrections are parametrically suppressed: The ones to the form factor relations enter with a suppression by small ratios of Wilson coefficients and the ones from subleading operators in the

OPE arise at $\mathcal{O}(\alpha_s)$ only. Moreover, the relevant hadronic matrix elements from both sources are not independent [10]. While the latter matrix elements are currently not known from first principles for $B \rightarrow K^*$, model estimates suggest that they are at least not enhanced beyond the naive expectations [12].

In this paper we extend previous works [14] on the low recoil region by allowing for BSM CP violation. We work to next-to-leading order (NLO) in QCD and to lowest order (LO) in $1/m_b$. The $\mathcal{O}(\Lambda_{\text{QCD}}/m_b)$ corrections are taken into account in the estimation of the uncertainties. Further higher order corrections, including charm loops with gluons are power-suppressed at low recoil [10, 11] and not considered given the targeted precision. The consistency between the outcome of an analysis excluding and using only the high- q^2 region data [14] supports the employed OPE framework.

We propose and study CP observables with only subleading form factor uncertainties in Sections II A and II B. In Section II C we calculate mixing-induced time-integrated CP asymmetries relevant for the decays $B_s, \bar{B}_s \rightarrow \phi(\rightarrow K^+K^-)l^+l^-$. In Section II D we give the relations between the CP observables and the angular distributions in $\bar{B} \rightarrow \bar{K}^*l^+l^-$ or likewise $\bar{B}_s \rightarrow \phi l^+l^-$ decays. We work out the constraints on the complex-valued short-distance coefficients in Section III and summarize in Section IV. In an appendix we present the method used to estimate the uncertainties from the $\mathcal{O}(\Lambda_{\text{QCD}}/m_b)$ corrections.

II. LOW RECOIL CP ASYMMETRIES

Our aim is to extend our previous study of $\Delta B = 1$ radiative and semileptonic decays [14] in the presence of CP violation. We use a model-independent framework with an effective Hamiltonian

$$\begin{aligned} \mathcal{H}_{\text{eff}} = & -\frac{G_{\text{F}}}{\sqrt{2}} \frac{e}{4\pi^2} V_{tb}V_{ts}^* \left(e\mathcal{C}_9 [\bar{s}\gamma_\mu P_L b] [\bar{l}\gamma^\mu l] + e\mathcal{C}_{10} [\bar{s}\gamma_\mu P_L b] [\bar{l}\gamma^\mu \gamma_5 l] \right. \\ & \left. + \mathcal{C}_7 m_b [\bar{s}\sigma^{\mu\nu} P_R b] F_{\mu\nu} \right) + \text{h.c.} + \dots, \end{aligned} \quad (2.1)$$

where the ellipses denote contributions which we assume to be SM-like because they are either subdominant in the radiative and semileptonic $b \rightarrow s$ decay amplitudes or induced in the SM at tree level. With CP violation beyond the SM, the Wilson coefficients \mathcal{C}_7 , \mathcal{C}_9 and \mathcal{C}_{10} are complex-valued. All other Wilson coefficients are assumed to be SM-like, and are real-valued after factoring out the Cabibbo-Kobayashi-Maskawa (CKM) factors V_{ik} , similar to Eq. (2.1). For details and definitions we refer to [14], which we follow closely. In particular, we take all numerical input as in [14] except for the CKM one, which we calculate from the Wolfenstein parameters $A = 0.812_{-0.027}^{+0.013}$,

$\lambda = 0.22543 \pm 0.00077$, $\bar{\rho} = 0.144 \pm 0.025$ and $\bar{\eta} = 0.342_{-0.015}^{+0.016}$ [15]. In the following we understand all Wilson coefficients to be evaluated at the scale $\mu_b \approx m_b$. The SM values of the most important ones are approximately, to next-to-next-to-leading logarithmic (NNLL) order,

$$\mathcal{C}_7^{\text{SM}} = -0.3, \quad \mathcal{C}_9^{\text{SM}} = 4.2, \quad \mathcal{C}_{10}^{\text{SM}} = -4.2. \quad (2.2)$$

A. Decay amplitudes with CP violation at low recoil

In a previous work [14] we identified

$$\rho_1 = \frac{1}{2} (|C^R|^2 + |C^L|^2) = \left| \mathcal{C}_9^{\text{eff}} + \kappa \frac{2\hat{m}_b}{\hat{s}} \mathcal{C}_7^{\text{eff}} \right|^2 + |\mathcal{C}_{10}|^2, \quad (2.3)$$

$$\rho_2 = \frac{1}{4} (|C^R|^2 - |C^L|^2) = \text{Re} \left\{ \left(\mathcal{C}_9^{\text{eff}} + \kappa \frac{2\hat{m}_b}{\hat{s}} \mathcal{C}_7^{\text{eff}} \right) \mathcal{C}_{10}^* \right\}, \quad (2.4)$$

as the only independent short-distance factors which enter the observables of the angular distribution of $\bar{B} \rightarrow \bar{K}^*(\rightarrow \bar{K}\pi)l^+l^-$ decays at low hadronic recoil. Here, $\hat{s} = q^2/m_B^2$ and $\hat{m}_b = m_b/m_B$, where m_B denotes the mass of the B meson. The factor κ accounts for the relation between the dipole ($T_{1,2,3}$) and (axial-) vector ($V, A_{1,2}$) form factors that can be calculated systematically [10, 12]. At lowest order in $1/m_b$ and including $\mathcal{O}(\alpha_s)$ corrections, it reads

$$\kappa = 1 - 2 \frac{\alpha_s}{3\pi} \ln \left(\frac{\mu}{m_b} \right). \quad (2.5)$$

The effective coefficients are written as

$$\mathcal{C}_7^{\text{eff}} = \mathcal{C}_7 - \frac{1}{3} \left[\mathcal{C}_3 + \frac{4}{3} \mathcal{C}_4 + 20 \mathcal{C}_5 + \frac{80}{3} \mathcal{C}_6 \right] + \frac{\alpha_s}{4\pi} \left[(\mathcal{C}_1 - 6 \mathcal{C}_2) A(q^2) - \mathcal{C}_8 F_8^{(7)}(q^2) \right], \quad (2.6)$$

and

$$\begin{aligned} \mathcal{C}_9^{\text{eff}} = & \mathcal{C}_9 + h(0, q^2) \left[\frac{4}{3} \mathcal{C}_1 + \mathcal{C}_2 + \frac{11}{2} \mathcal{C}_3 - \frac{2}{3} \mathcal{C}_4 + 52 \mathcal{C}_5 - \frac{32}{3} \mathcal{C}_6 \right] \\ & - \frac{1}{2} h(m_b, q^2) \left[7 \mathcal{C}_3 + \frac{4}{3} \mathcal{C}_4 + 76 \mathcal{C}_5 + \frac{64}{3} \mathcal{C}_6 \right] + \frac{4}{3} \left[\mathcal{C}_3 + \frac{16}{3} \mathcal{C}_5 + \frac{16}{9} \mathcal{C}_6 \right] \\ & + \frac{\alpha_s}{4\pi} \left[\mathcal{C}_1 (B(q^2) + 4C(q^2)) - 3 \mathcal{C}_2 (2B(q^2) - C(q^2)) - \mathcal{C}_8 F_8^{(9)}(q^2) \right] \\ & + 8 \frac{m_c^2}{q^2} \left[\left(\frac{4}{9} \mathcal{C}_1 + \frac{1}{3} \mathcal{C}_2 \right) (1 + \hat{\lambda}_u) + 2 \mathcal{C}_3 + 20 \mathcal{C}_5 \right], \end{aligned} \quad (2.7)$$

where we extended previous works [10, 14] by including the doubly Cabibbo-suppressed contribution proportional to $\hat{\lambda}_u = V_{ub}V_{us}^*/(V_{tb}V_{ts}^*)$. The latter is responsible for CP violation in the SM and appears only in the coefficient $\mathcal{C}_9^{\text{eff}}$ with m_c^2/q^2 suppression. We refer to [10, 14] for more details

concerning the (real-valued) Wilson coefficients $\mathcal{C}_{i \leq 6}$ as well as the LO and NLO QCD corrections encoded in the functions $h(m_i, q^2)$ and $A, B, C, F_8^{(7,9)}$, respectively.

In the presence of CP violation, there are four independent short-distance factors

$$\rho_1, \rho_2 \quad \text{and} \quad \bar{\rho}_1, \bar{\rho}_2, \quad (2.8)$$

where the barred factors are obtained from the unbarred ones by complex conjugation of the Wilson coefficients \mathcal{C}_i and the CKM factor $\hat{\lambda}_u$. The building blocks describing CP violation are hence

$$\Delta\rho_i = \rho_i - \bar{\rho}_i \quad \text{with} \quad i = 1, 2. \quad (2.9)$$

They can be written as

$$\Delta\rho_1 = 4 \text{Im} Y \cdot \text{Im} \left\{ \mathcal{C}_9 + \kappa \frac{2\hat{m}_b}{\hat{s}} \mathcal{C}_7 + Y_9^{(u)} \hat{\lambda}_u \right\}, \quad (2.10)$$

$$\Delta\rho_2 = 2 \text{Im} Y \cdot \text{Im} \mathcal{C}_{10}, \quad (2.11)$$

using

$$Y = Y_9 + \kappa \frac{2\hat{m}_b}{\hat{s}} Y_7 \quad (2.12)$$

and the decomposition of Eqs. (2.6) and (2.7) into

$$\mathcal{C}_7^{\text{eff}} = \mathcal{C}_7 + Y_7, \quad \mathcal{C}_9^{\text{eff}} = \mathcal{C}_9 + Y_9 + \hat{\lambda}_u Y_9^{(u)}. \quad (2.13)$$

Note that $Y_9^{(u)}$ is real-valued, and we suppress the q^2 -dependence in the effective coefficients and the Y_i throughout this work. It follows from Eqs. (2.10)-(2.11) that $\Delta\rho_1$ probes the weak phases of \mathcal{C}_7 and \mathcal{C}_9 , whereas $\Delta\rho_2$ probes the weak phase of \mathcal{C}_{10} . The imaginary parts of the Y_i give rise to the strong phases and hence drive the magnitude of CP violation.

In Fig. 1 we show the imaginary part of Y_9 (dashed curve) and Y (solid curve) from the OPE [10] at NLO QCD using Eqs. (2.6) and (2.7). The NLO QCD corrections to both $\text{Im} Y_{7,9}$ are sizeable and lead to a reduction of the strong phases compared to the LO value of $\text{Im} Y$ (dashed-dotted curve). Since $\text{Im} Y_7$ vanishes at LO, the NLO corrections constitute the leading contribution to this quantity.

Also shown in Fig. 1 is the absorptive part $\text{Im} Y^{c\bar{c}}$ (dotted curve) obtained from a phenomenological fit to $e^+e^- \rightarrow \text{hadrons}$ data assuming factorization [16]. The Breit-Wigner amplitude matches the charmonium peaks of the branching ratios $\mathcal{B}(\bar{B} \rightarrow \bar{K}^* c\bar{c})$ for $c\bar{c} = J/\Psi$ and Ψ' . Note that for NNLL values of the Wilson coefficients \mathcal{C}_1 and \mathcal{C}_2 and with present day data [17] no fudge factor [18] is needed. We apply this ansatz for the higher $c\bar{c}$ -resonances as well, where presently no B -decay data

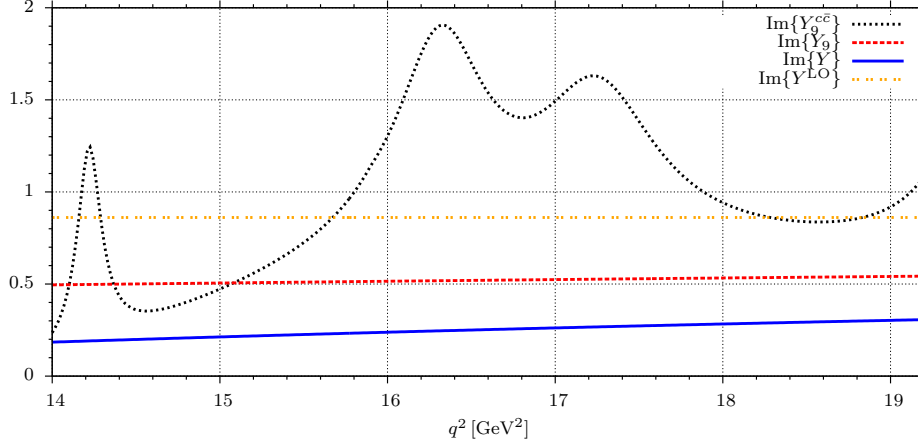


FIG. 1: The imaginary parts of Y (solid, blue) and Y_9 (dashed, red) in the OPE [10] including NLO α_s -corrections as functions of q^2 in the low recoil region. The LO result, where $\text{Im} Y = \text{Im} Y_9$ is shown by the dashed-dotted (orange) curve. The $c\bar{c}$ -resonance curve (dotted, black) shows the imaginary part of Y_9 from $e^+e^- \rightarrow \text{hadrons}$ data [16, 17].

exist. The fit exhibits the local charm resonance structure from $\bar{B} \rightarrow \bar{K}^*(c\bar{c}) \rightarrow \bar{K}^*l^+l^-$ decays. As can be seen in Fig. 1, the resonance contribution is of the same order as the OPE prediction at LO QCD and indicates comparable results after integrating over a sufficiently large region in the dilepton mass. However, we find a factor of ~ 3 between both approaches when using NLO QCD corrections and integrating over the low recoil region.

B. The low recoil CP asymmetries

At low recoil and within our framework (LO in $1/m_b$, SM operator basis Eq. (2.1)) all $\bar{B} \rightarrow \bar{K}^*l^+l^-$ observables are, as far as short-distance physics is concerned, either proportional to ρ_1 , ρ_2/ρ_1 or short-distance insensitive [14]. Consequently, there are only two types of CP asymmetries:

$$a_{\text{CP}}^{(1)} \equiv \frac{\rho_1 - \bar{\rho}_1}{\rho_1 + \bar{\rho}_1}, \quad a_{\text{CP}}^{(2)} \equiv \frac{\frac{\rho_2}{\rho_1} - \frac{\bar{\rho}_2}{\bar{\rho}_1}}{\frac{\rho_2}{\rho_1} + \frac{\bar{\rho}_2}{\bar{\rho}_1}}. \quad (2.14)$$

It is advantageous to define further

$$a_{\text{CP}}^{(3)} \equiv 2 \frac{\rho_2 - \bar{\rho}_2}{\rho_1 + \bar{\rho}_1}, \quad (2.15)$$

which is not independent of $a_{\text{CP}}^{(1,2)}$. Since $(\rho_1 + \bar{\rho}_1)$ is positive definite, see Eq. (2.3), it is in general better suited for normalisation than the denominator of $a_{\text{CP}}^{(2)}$, which might cross zero and could make the theoretical uncertainties blow up. We note that $a_{\text{CP}}^{(1)}$ equals the direct CP asymmetry in

the rate, $A_{\text{CP}} \equiv \frac{\Gamma - \bar{\Gamma}}{\Gamma + \bar{\Gamma}}$. Furthermore, $a_{\text{CP}}^{(2)}$ equals $A_{\text{FB}}^{\text{CP}} \equiv \frac{A_{\text{FB}} + \bar{A}_{\text{FB}}}{A_{\text{FB}} - \bar{A}_{\text{FB}}}$ [19], the CP asymmetry of the forward-backward asymmetry, whereas $a_{\text{CP}}^{(3)}$ corresponds to the low recoil transversity observables $H_T^{(2,3)}$ introduced in Ref. [14]. No further CP asymmetries can be formed from the decays at low recoil beyond Eqs. (2.14)-(2.15) unless one considers neutral meson mixing, which we do in the next section. Note that $a_{\text{CP}}^{(1,2)}$ are related to observables which require B -flavour tagging, whereas $a_{\text{CP}}^{(3)}$ can be extracted from untagged B meson samples [cf. Section IID].

Using $\Delta\rho_i \ll \rho_i, \bar{\rho}_i$ the expressions for the CP asymmetries simplify to

$$a_{\text{CP}}^{(1)} \approx \frac{\Delta\rho_1}{2\rho_1}, \quad a_{\text{CP}}^{(2)} \approx \frac{\Delta\rho_2}{2\rho_2} - a_{\text{CP}}^{(1)}, \quad a_{\text{CP}}^{(3)} \approx \frac{\Delta\rho_2}{\rho_1}. \quad (2.16)$$

The SM values of the CP asymmetries are induced at the order $(m_c^2/m_b^2) \text{Im}\hat{\lambda}_u \sim 10^{-3}$ and are tiny. Since the CP asymmetries at low recoil are T-even only, a finite strong phase is needed for a finite CP asymmetry. The strong phase is roughly given as $\arg(Y)$, yielding an additional suppression by another order of magnitude. Therefore, at low recoil

$$\left| a_{\text{CP}}^{(1,2,3)} \right|_{\text{SM}} \lesssim 10^{-4}. \quad (2.17)$$

Given the foreseen experimental precision, the CP asymmetries in the SM are therefore completely negligible due to their strong parametric suppression. Hence, any observed finite CP asymmetry is a signal of physics beyond the SM.

Beyond the SM, the CP asymmetries at low recoil can be significantly enhanced. To estimate the order of magnitude of $a_{\text{CP}}^{(1,2,3)}$ we assume that $|\mathcal{C}_{7,9,10}|$ are close to their respective SM values where $|\mathcal{C}_7^{\text{SM}}| \ll |\mathcal{C}_{9,10}^{\text{SM}}|$. Then, using Eq. (2.16) and $\text{Im} Y$ as shown in Fig. 1, we obtain, roughly,

$$a_{\text{CP}}^{(1)} \simeq \frac{2 \text{Im} Y}{|\mathcal{C}_9|^2 + |\mathcal{C}_{10}|^2} \text{Im} \left(\mathcal{C}_9 + \kappa \frac{2\hat{m}_b}{\hat{s}} \mathcal{C}_7 \right) \lesssim \mathcal{O}(0.1), \quad (2.18)$$

$$a_{\text{CP}}^{(2)} \simeq \frac{\text{Im} Y \text{Im} \mathcal{C}_{10}}{\text{Re} \mathcal{C}_9 \mathcal{C}_{10}^*} - a_{\text{CP}}^{(1)} \lesssim \mathcal{O}(0.1), \quad (2.19)$$

$$a_{\text{CP}}^{(3)} \simeq \frac{\text{Im} Y \text{Im} \mathcal{C}_{10}}{|\mathcal{C}_9|^2 + |\mathcal{C}_{10}|^2} \lesssim \mathcal{O}(0.1), \quad (2.20)$$

in agreement with [19–21]. Note that for very small BSM values of $\text{Re} \mathcal{C}_9 \mathcal{C}_{10}^*$ the values of $a_{\text{CP}}^{(2)}$ become unconstrained. Furthermore, for $\text{Im} \mathcal{C}_{10} = 0$ the following relations hold

$$a_{\text{CP}}^{(1)} = -a_{\text{CP}}^{(2)}, \quad a_{\text{CP}}^{(3)} = 0. \quad (2.21)$$

To investigate more quantitatively the above CP asymmetries we define a BSM benchmark point

$$\mathcal{C}_7 = -0.3i, \quad \mathcal{C}_9 = +4.2i, \quad \mathcal{C}_{10} = -4.2i, \quad (2.22)$$

	LO	NLO	$c\bar{c}$ -resonances
$\langle a_{\text{CP}}^{(1)} \rangle$	$+0.208 \begin{smallmatrix} +0.036 \\ -0.050 \end{smallmatrix} \Big _{\text{SD}} \pm 0.006 \Big _{\text{SL}}$	$+0.074 \begin{smallmatrix} +0.029 \\ -0.037 \end{smallmatrix} \Big _{\text{SD}} \pm 0.011 \Big _{\text{SL}}$	+0.17
$\langle a_{\text{CP}}^{(2)} \rangle$	$+0.071 \begin{smallmatrix} +0.016 \\ -0.015 \end{smallmatrix} \Big _{\text{SD}} \pm 0.009 \Big _{\text{SL}}$	$+0.020 \begin{smallmatrix} +0.005 \\ -0.008 \end{smallmatrix} \Big _{\text{SD}} \pm 0.006 \Big _{\text{SL}}$	+0.06
$\langle a_{\text{CP}}^{(3)} \rangle$	$-0.257 \begin{smallmatrix} +0.056 \\ -0.035 \end{smallmatrix} \Big _{\text{SD}} \pm 0.009 \Big _{\text{SL}}$	$-0.090 \begin{smallmatrix} +0.044 \\ -0.031 \end{smallmatrix} \Big _{\text{SD}} \pm 0.010 \Big _{\text{SL}}$	-0.20

TABLE I: The q^2 -integrated low recoil CP asymmetries at LO and NLO QCD for the BSM benchmark point (cf. Eq. (2.22)) with the main uncertainties from the variation of the renormalisation scale μ_b (SD) and subleading power corrections (SL). Also given are the asymmetries using $c\bar{c}$ -resonance data [16, 17].

which passes all the current experimental constraints. In particular, both interference terms $\text{Re } \mathcal{C}_9 \mathcal{C}_{10}^*$ and $\text{Re } \mathcal{C}_9 \mathcal{C}_7^*$ which are probed by $A_{\text{FB}}(\bar{B} \rightarrow \{X_s, \bar{K}^*\} l^+ l^-)$ and the $\bar{B} \rightarrow \{X_s, \bar{K}^{(*)}\} l^+ l^-$ branching ratios, respectively, are SM-like. Due to the maximal phases the benchmark values induce large BSM CP violation. The CP asymmetries evaluated at the benchmark point are given in Table I. Throughout this work we use $\langle \dots \rangle$ to denote the integrated observables formed out of integrated angular coefficients following Ref. [14]. For the low recoil integration region we take $14 \text{ GeV}^2 < q^2 \leq 19.2 \text{ GeV}^2$. We find that the main parametric uncertainty in $\langle a_{\text{CP}}^{(i)} \rangle$ stems from the variation of the renormalisation scale $\mu_b \in [2.1, 8.4] \text{ GeV}$ (SD). When varying the scale μ_b , the model-independent BSM contributions to the Wilson coefficients Eq. (2.22) are assumed to be given at the reference scale $\mu = 4.2 \text{ GeV}$ and their renormalisation group evolution to μ_b is taken into account in leading logarithmic approximation. While an efficient cancellation of the μ_b -dependence is at work in the sum $\mathcal{C}_i^{\text{eff}} = \mathcal{C}_i + Y_i$, the numerators of the CP asymmetries depend on the product of $\text{Im } \mathcal{C}_i$ and $\text{Im } Y$, and result in the large reported uncertainties. The subleading corrections to the Isgur-Wise form factor relations and transversity amplitudes (SL) constitute another major source of uncertainty. Its estimate is explained in Appendix A.

As can be seen from Table I the impact of the NLO corrections is sizable on the CP asymmetries. The LO predictions are about a factor 3 larger than the NLO ones due to large destructive NLO contributions to $\text{Im } Y$. In fact, concerning $\text{Im } Y_7$ the NLO corrections constitute the leading contribution which also implies a large scale uncertainty at NLO, but the NLO corrections are sizeable in $\text{Im } Y_9$, too.

Also shown in Table I are the CP asymmetries calculated using a phenomenological ansatz with $c\bar{c}$ -resonances [16, 17]. They are in the general ballpark of the OPE ones, between the LO and NLO findings, and somewhat smaller than the LO results.

C. Untagged CP asymmetries with meson mixing

We consider the decays $B_s, \bar{B}_s \rightarrow \phi(\rightarrow K^+K^-)l^+l^-$ which especially for muons are of great importance for hadron collider experiments. We follow closely [4] to which we refer for details on the full angular distribution [1].

To account for neutral meson mixing, time-dependent transversity amplitudes need to be introduced:

$$\begin{aligned} A_a^{L/R}(t) &\equiv A^{L/R}(\bar{B}_s(t) \rightarrow \phi(\rightarrow K^+K^-)_a l^+l^-), \\ \bar{A}_a^{L/R}(t) &\equiv A^{L/R}(B_s(t) \rightarrow \phi(\rightarrow K^+K^-)_a l^+l^-), \end{aligned} \quad (2.23)$$

where $A_a^{L/R}(t), (\bar{A}_a^{L/R}(t))$ denotes the amplitude for a meson born at time $t = 0$ as a $\bar{B}_s, (B_s)$ decaying through the transversity amplitude $a = \perp, \parallel, 0$ at later times t .

For the time evolution the following parameters which involve the un-mixed amplitudes at $t = 0$ play an important role

$$\xi_a^{L/R} = e^{-i\Phi_M} \frac{A_a^{L/R}(0)}{A_a^{L/R}(0)[\delta_W \rightarrow -\delta_W]}, \quad (2.24)$$

where $[\delta_W \rightarrow -\delta_W]$ implies the conjugation of all weak phases in the denominator. Here Φ_M denotes the phase of the $B_s - \bar{B}_s$ mixing amplitude which is very small in the SM, $\Phi_M^{\text{SM}} = 2 \arg(V_{ts}^* V_{tb})$.

The untagged rates $d\Gamma + d\bar{\Gamma}$ can then be written as [22]

$$\begin{aligned} \bar{A}_a(t)\bar{A}_b^*(t) + A_a(t)A_b^*(t) &= \frac{1}{2}\bar{A}_a(0)\bar{A}_b^*(0) \\ &\times [(1 + \eta_a\eta_b \xi_a\xi_b^*) (e^{-\Gamma_L t} + e^{-\Gamma_H t}) + (\eta_a\xi_a + \eta_b\xi_b^*) (e^{-\Gamma_L t} - e^{-\Gamma_H t})], \end{aligned} \quad (2.25)$$

where the chirality indices L, R are suppressed for brevity. Here, $\eta_{0,\parallel} = +1$ and $\eta_{\perp} = -1$ are the CP eigenvalues of the final state and $\Gamma_{L(H)}$ denotes the width of the lighter (heavier) mass eigenstate of the B_s system. We also neglect CP violation in mixing, which is bounded by the semileptonic asymmetry for B_s mesons $|A_{\text{SL}}^s| \lesssim \mathcal{O}(10^{-2})$ [23].

After time-integration follows from Eq. (2.25)

$$\int_0^\infty dt [\bar{A}_a(t)\bar{A}_b^*(t) + A_a(t)A_b^*(t)] = \frac{\bar{A}_a(0)\bar{A}_b^*(0)}{\Gamma(1-y^2)} [1 + \eta_a\eta_b \xi_a\xi_b^* - y(\eta_a\xi_a + \eta_b\xi_b^*)], \quad (2.26)$$

where $\Gamma = (\Gamma_L + \Gamma_H)/2$ and $\Delta\Gamma = \Gamma_L - \Gamma_H$ denote the average width and the width difference, respectively, and $y = \Delta\Gamma/(2\Gamma)$.

Due to the simple transversity structure at low recoil [14], see Eq. (1.1), there are only two different time evolution parameters, ξ_L and ξ_R , universal for all the $\perp, \parallel, 0$ amplitudes. We obtain

$$\xi_{L/R} = e^{-i\Phi_M} \frac{\mathcal{C}_9 \mp \mathcal{C}_{10} + \kappa \frac{2\hat{m}_b}{\hat{s}} \mathcal{C}_7 + Y + \hat{\lambda}_u Y_9^{(u)}}{\mathcal{C}_9^* \mp \mathcal{C}_{10}^* + \kappa \frac{2\hat{m}_b}{\hat{s}} \mathcal{C}_7^* + Y + \hat{\lambda}_u^* Y_9^{(u)}}. \quad (2.27)$$

In the absence of strong phases we find $|\xi_{L/R}| = 1$ and in the absence of CP violation in the rare decays holds $|\xi_{L/R}| = 1$ as well. In the SM, CP violation in these parameters is very small: $|\xi_{L/R}| - 1 = \mathcal{O}\left((m_c^2/m_b^2) \text{Im } \hat{\lambda}_u\right)$.

CP-odd observables allow to measure CP violation without tagging the flavour of the initial B meson (if the asymmetry between B_s and \bar{B}_s production is known). Among the available coefficients in the angular distribution four of them, $J_{5,6,8,9}$, are CP-odd [1, 4]. However, in the low recoil region the coefficients $J_{7,8,9}$ vanish [14], leaving only $J_{5,6}$ for untagged CP measurements.

For J_5 we obtain at low recoil from Eq. (2.26):

$$\int_0^\infty dt \text{Re} \left\{ \bar{A}_0^L(t) \bar{A}_\perp^{L,*}(t) + A_0^L(t) A_\perp^{L,*}(t) - (L \rightarrow R) \right\} = f_0 f_\perp \times \frac{A_{mix}}{\Gamma(1-y^2)} \quad (2.28)$$

with

$$A_{mix} = 2\rho_2(|\xi_L|^2 + |\xi_R|^2 - 2) + \rho_1(|\xi_R|^2 - |\xi_L|^2). \quad (2.29)$$

The formula for J_6 is identical after changing the transversity index 0 to \parallel .

In order to reduce non-perturbative uncertainties, we choose combinations of the following untagged, time-integrated quantities for normalisation:

$$n_i = \int_0^\infty dt \left[|\bar{A}_i^L(t)|^2 + |A_i^L(t)|^2 + (L \rightarrow R) \right] = f_i^2 \times \frac{(B_{mix} - 2\eta_i y C_{mix})}{\Gamma(1-y^2)}, \quad (2.30)$$

which can be obtained from the angular observables $J_{1,2,3}$. Here,

$$B_{mix} = \rho_1(|\xi_L|^2 + |\xi_R|^2 + 2) + 2\rho_2(|\xi_R|^2 - |\xi_L|^2), \quad (2.31)$$

$$C_{mix} = \rho_1 \text{Re}\{\xi_L + \xi_R\} + 2\rho_2 \text{Re}\{\xi_R - \xi_L\}. \quad (2.32)$$

Note that C_{mix} only depends on the mixing phase Φ_M .

Normalizing Eq. (2.28) to $\sqrt{n_\perp n_0}$ yields a mixing-induced analogue of $a_{\text{CP}}^{(3)}$:

$$a_{\text{CP}}^{mix} = \frac{A_{mix}}{\sqrt{(B_{mix})^2 - 4y^2 (C_{mix})^2}}. \quad (2.33)$$

Note that at low recoil a_{CP}^{mix} is insensitive to the sign of y . Simultaneously, the sensitivity to Φ_M is very low since it enters via C_{mix} only. In the limit $y \rightarrow 0$ holds

$$a_{\text{CP}}^{mix} = \frac{A_{mix}}{|B_{mix}|} = -2 \frac{(\rho_1^2 + 4\rho_2^2)\bar{\rho}_2 - 2\rho_1\rho_2\bar{\rho}_1 + (\bar{\rho}_1^2 - 4\bar{\rho}_2^2)\rho_2}{(\rho_1^2 + 4\rho_2^2)\bar{\rho}_1 - 8\rho_1\rho_2\bar{\rho}_2 + (\bar{\rho}_1^2 - 4\bar{\rho}_2^2)\rho_1}. \quad (2.34)$$

For $\Delta\rho_i \ll \rho_i, \bar{\rho}_i$ this simplifies further to

$$a_{\text{CP}}^{\text{mix}} = a_{\text{CP}}^{(3)}. \quad (2.35)$$

The use of the coefficient J_6 with normalization to $\sqrt{n_{\parallel}n_{\perp}}$ leads to a second possibility to measure the very same asymmetry $a_{\text{CP}}^{\text{mix}}$.

The sensitivity to the B_s -mixing parameters y and Φ_M is low for realistic values of $y \lesssim \mathcal{O}(0.1)$. We find for the q^2 -integrated asymmetries that, model-independently, $|\langle a_{\text{CP}}^{\text{mix}} \rangle / \langle a_{\text{CP}}^{(3)} \rangle - 1|$ is below a few percent and hence unlikely to be measured in the foreseen future.

D. CP asymmetries from the angular distribution

Here we summarise the relations between the low recoil CP asymmetries $a_{\text{CP}}^{(1,2,3)}$ and the CP asymmetries studied previously in the literature. We begin by showing various possibilities to extract the $a_{\text{CP}}^{(i)}$ from the angular distribution. We neglect the small corrections from finite lepton masses m_l in kinematical factors $\beta_l = \sqrt{1 - 4m_l^2/q^2}$.

As already mentioned, $a_{\text{CP}}^{(1)}$ equals the total rate asymmetry A_{CP} given as

$$a_{\text{CP}}^{(1)} = A_{\text{CP}} = \frac{\Gamma - \bar{\Gamma}}{\Gamma + \bar{\Gamma}}. \quad (2.36)$$

Here, form factor uncertainties cancel at low recoil.

The asymmetry $a_{\text{CP}}^{(2)}$ can be extracted in a multitude of ways from the ratios

$$a_{\text{CP}}^{(2)} = \frac{R_{ab} - \bar{R}_{ab}}{R_{ab} + \bar{R}_{ab}}, \quad R_{ab} = \frac{\sum_a c_a J_a}{\sum_b c_b J_b}, \quad \bar{R}_{ab} = R_{ab}[J_i \rightarrow \pm \bar{J}_i], \quad (2.37)$$

which provides a cancellation of the form factor uncertainties in the low recoil region. The “+” and “-” sign in the third relation apply for CP-even $i = 1, 2, 3, 4$ and CP-odd $i = 5, 6$ coefficients J_i in the angular decay distribution, respectively. The ratios R_{ab} can have $a = 5, 6$ and $b = 1, 2, 3, 4$ and the c_i are auxiliary real numbers. For example, $A_{\text{FB}}^{\text{CP}}$ can be recovered for $\sum_a c_a J_a = J_6$ and $\sum_b c_b J_b = J_1 - J_2/3$ (with $J_{1,2} \equiv 2J_{1,2}^s + J_{1,2}^c$)

$$a_{\text{CP}}^{(2)} = A_{\text{FB}}^{\text{CP}} = \frac{A_{\text{FB}} + \bar{A}_{\text{FB}}}{A_{\text{FB}} - \bar{A}_{\text{FB}}}. \quad (2.38)$$

The CP asymmetries $A_i \equiv 2(J_i - \bar{J}_i)/d(\Gamma + \bar{\Gamma})/dq^2$ and $A_i^D \equiv -2(J_i - \bar{J}_i)/d(\Gamma + \bar{\Gamma})/dq^2$ defined in [4] are related in the low recoil region to the CP asymmetries $a_{\text{CP}}^{(1,3)}$ as

$$\begin{aligned} A_3 &= a_{\text{CP}}^{(1)} \times \frac{3}{4} \frac{f_{\perp}^2 - f_{\parallel}^2}{f_{\perp}^2 + f_{\parallel}^2 + f_0^2}, & A_4^D &= -a_{\text{CP}}^{(1)} \times \frac{3}{\sqrt{8}} \frac{f_0 f_{\parallel}}{f_{\perp}^2 + f_{\parallel}^2 + f_0^2}, \\ A_5^D &= -a_{\text{CP}}^{(3)} \times \frac{3}{\sqrt{2}} \frac{f_0 f_{\perp}}{f_{\perp}^2 + f_{\parallel}^2 + f_0^2}, & A_6 &= a_{\text{CP}}^{(3)} \times 3 \frac{f_{\perp} f_{\parallel}}{f_{\perp}^2 + f_{\parallel}^2 + f_0^2}, \end{aligned} \quad (2.39)$$

whereas $A_{7,8,9}^{(D)}$ vanish. Unlike in $a_{\text{CP}}^{(1,2,3)}$ in the asymmetries Eq. (2.39) the form factors do not drop out and the corresponding uncertainties do not cancel.

The CP asymmetry $a_{\text{CP}}^{(3)}$ is identical to the low recoil transversity observables $H_T^{(2)}$ and $H_T^{(3)}$ [14] when measuring them in an untagged sample containing an equal number of \bar{B} and B mesons

$$a_{\text{CP}}^{(3)} = \begin{cases} \frac{J_5 - \bar{J}_5}{\sqrt{-2(J_2^c + \bar{J}_2^c)[2(J_2^s + \bar{J}_2^s) + (J_3 + \bar{J}_3)]}} & \text{for } H_T^{(2)} \\ \frac{J_6 - \bar{J}_6}{2\sqrt{4(J_2^s + \bar{J}_2^s)^2 - (J_3 + \bar{J}_3)^2}} & \text{for } H_T^{(3)}. \end{cases} \quad (2.40)$$

The mixing-induced, time-integrated CP asymmetries A_5^{Dmix} and A_6^{mix} defined in [4] are related to a_{CP}^{mix} as follows

$$A_5^{Dmix} = -a_{\text{CP}}^{mix} \times \frac{3}{\sqrt{2}} \frac{n_0 n_{\perp}}{n_{\perp}^2 + n_{\parallel}^2 + n_0^2}, \quad A_6^{mix} = a_{\text{CP}}^{mix} \times 3 \frac{n_{\perp} n_{\parallel}}{n_{\perp}^2 + n_{\parallel}^2 + n_0^2}, \quad (2.41)$$

where the n_i have been introduced in Eq. (2.30). As in Eq. (2.39), and unlike in a_{CP}^{mix} , the asymmetries given in Eq. (2.41) exhibit a residual form factor dependence.

Ways to extract the angular coefficients J_i from the full differential decay distribution have been given in Ref. [4], to which we refer for details and the definitions of the kinematic angles θ_l, θ_{K^*} and ϕ . For example, J_6 requires two bins, $\cos \theta_l \in [-1, 0]$ and $[0, 1]$, while J_5 can be extracted from the single-differential distribution in the angle ϕ with additional bins, $\cos \theta_{K^*} \in [-1, 0]$ and $[0, 1]$.

III. MODEL-INDEPENDENT $\Delta B = 1$ CONSTRAINTS

We perform a global analysis of the available $b \rightarrow sl^+l^-$ decay data in the presence of BSM CP violation through the Wilson coefficients $\mathcal{C}_{7,9,10}$, i.e., allowing them to be complex-valued. We follow the same approach and the same data sources as presented in [14] to perform a six-dimensional scan of the magnitudes $|\mathcal{C}_{7,9,10}|$ and phases $\phi_{7,9,10} \equiv \arg \mathcal{C}_{7,9,10}$. We use the following ranges and binning

$$\begin{aligned} |\mathcal{C}_7| \in [0.30, 0.35] & \quad \Delta|\mathcal{C}_7| = 0.01, & \phi_7 \in [0, 2\pi] & \quad \Delta\phi_7 = \frac{\pi}{16}, \\ |\mathcal{C}_9| \in [0, 15] & \quad \Delta|\mathcal{C}_9| = 0.25, & \phi_9 \in [0, 2\pi] & \quad \Delta\phi_9 = \frac{\pi}{16}, \\ |\mathcal{C}_{10}| \in [0, 15] & \quad \Delta|\mathcal{C}_{10}| = 0.25, & \phi_{10} \in [0, 2\pi] & \quad \Delta\phi_{10} = \frac{\pi}{16}. \end{aligned} \quad (3.1)$$

The narrow range for $|\mathcal{C}_7| \approx |\mathcal{C}_7^{\text{SM}}|$ is justified by the good agreement of the measured $\bar{B} \rightarrow X_s \gamma$ branching ratio with its SM prediction [24, 25]. For the scan we used and developed further EOS [26], a program for the evaluation of flavour observables.

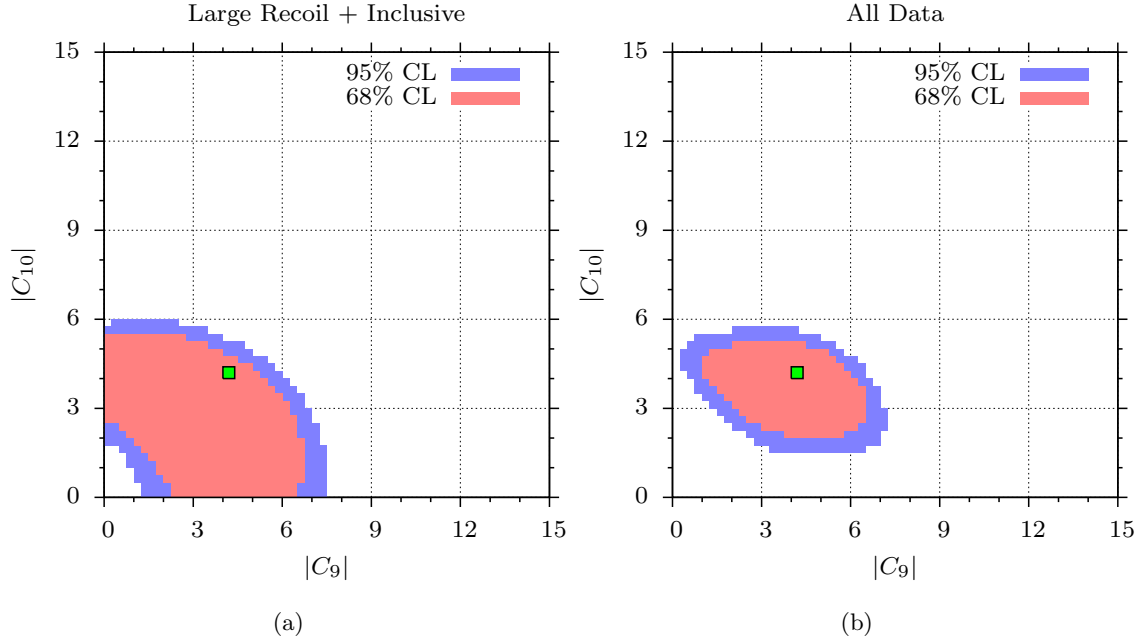


FIG. 2: The constraints on $|\mathcal{C}_9|$ and $|\mathcal{C}_{10}|$ from the experimental data as collected in [14]. The areas correspond to 68% CL (red) and 95% CL intervals (blue). In the left plot (a), data from the low recoil region has been excluded, while the right plot (b) has been obtained using the full set of available data. The (light green) square marks the SM.

In order to visualize the constraints, we project the 68% and 95% confidence regions of the six-dimensional scan onto the $|\mathcal{C}_9|$ - $|\mathcal{C}_{10}|$ plane, shown in Fig. 2. The projections onto $|\mathcal{C}_9|$ - ϕ_9 , $|\mathcal{C}_{10}|$ - ϕ_{10} and ϕ_9 - ϕ_{10} are obtained likewise, and are shown in Fig. 3. The data from $\bar{B} \rightarrow \bar{K}^* l^+ l^-$ decays in the low recoil region provide powerful additional constraints as can be seen by comparing the results with or without including them. We find good agreement between the SM and the data.

The scan procedure returns the allowed ranges, see Fig. 2,

$$\begin{aligned}
 1.0 \leq |\mathcal{C}_9| \leq 6.5 & & (0.3 \leq |\mathcal{C}_9| \leq 7.3), \\
 2.0 \leq |\mathcal{C}_{10}| \leq 5.3 & & (1.5 \leq |\mathcal{C}_{10}| \leq 5.8),
 \end{aligned}
 \tag{3.2}$$

at 68% CL (95% CL). Due to its smallness the above finite lower 95% CL-bound on $|\mathcal{C}_9|$ is sensitive to the discretisation of the scan, $\Delta|\mathcal{C}_9| = 0.25$, and is subject to corresponding uncertainties.

From Eqs. (2.2) and (3.2) we find for the branching ratio of the decay $\bar{B}_s \rightarrow \mu^+ \mu^-$ with respect to its SM value a maximal enhancement by a factor 1.9. Employing for the decay constant of the B_s meson $f_{B_s} = 231(15)(4)$ MeV [27], we obtain the 95% CL upper limit $\mathcal{B}(\bar{B}_s \rightarrow \mu^+ \mu^-) < 8 \times 10^{-9}$. The corresponding SM value is given as $\mathcal{B}(\bar{B}_s \rightarrow \mu^+ \mu^-)_{\text{SM}} = (3.1 \pm 0.6) \times 10^{-9}$ with the dominant

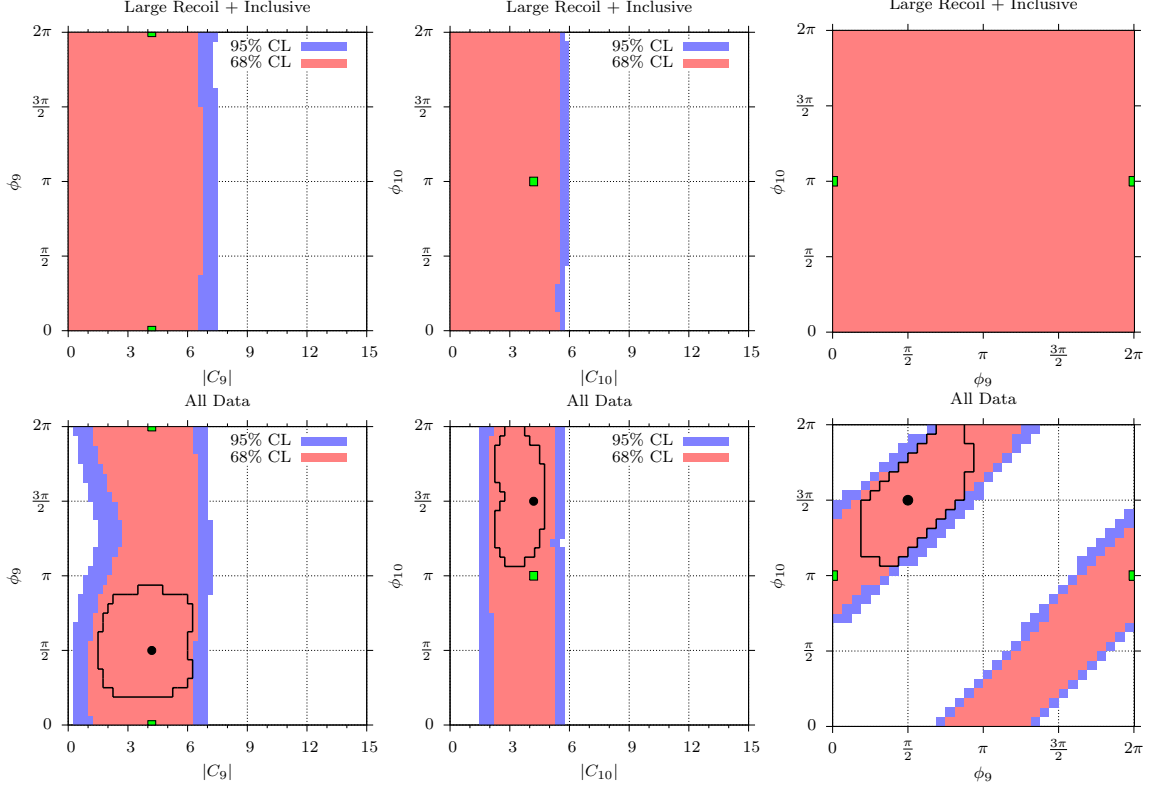


FIG. 3: The constraints on complex-valued \mathcal{C}_9 and \mathcal{C}_{10} from the experimental data as collected in [14]. The areas correspond to 68% CL (red) and 95% CL intervals (blue). The upper row shows the constraints using the large recoil region of the exclusive and inclusive decays only. In the lower row, all data from both the low and the large recoil regions are used. The solid (black) lines mark the 68% CL regions obtained by employing in addition a hypothetical measurement of $\langle a_{\text{CP}}^{(1)} \rangle = 0.074 \pm 0.01$ with a central value corresponding to the one at the BSM benchmark point (cf. Eq. (2.22)). The (light green) square denotes the SM value of $(\mathcal{C}_9, \mathcal{C}_{10})$, while the benchmark point is denoted by the black circle.

uncertainty stemming from the decay constant. Using $f_{B_s} = 256(6)(6)$ MeV [28], we obtain a slightly larger upper limit $\mathcal{B}(\bar{B}_s \rightarrow \mu^+ \mu^-) < 9 \times 10^{-9}$, and $\mathcal{B}(\bar{B}_s \rightarrow \mu^+ \mu^-)_{\text{SM}} = (3.8 \pm 0.4) \times 10^{-9}$. The SM region of $\bar{B}_s \rightarrow \mu^+ \mu^-$ decays will be at least partially accessed by the LHCb experiment with the 2011-2012 LHC run with projected luminosity up to around 2 fb^{-1} [29].

We find the approximate 95% CL ranges for the phases, see Fig. 3,

$$\frac{\pi}{2} \lesssim \arg(\mathcal{C}_9 \mathcal{C}_{10}^*) \lesssim \frac{3\pi}{2}, \quad (3.3)$$

with corresponding 2π -periodic branches. We note that the experimental information entering our scans stems from CP-conserving data only and the constraints on the BSM phases are currently weak. While the B -factories already measured the rate asymmetry of $\bar{B} \rightarrow \bar{K}^* l^+ l^-$ decays at the

level of $\mathcal{O}(0.1)$ [23], these constraints are not included in our analysis because they are given for the total integrated rate only, or are inappropriately binned such as the high q^2 rate asymmetry measurement by BaBar, $A_{\text{CP}} = 0.09 \pm 0.21 \pm 0.02$, given for $q^2 > 10.24 \text{ GeV}^2$ and excluding the Ψ' -peak [30]. We checked explicitly that an $\langle a_{\text{CP}}^{(1)} \rangle$ measurement at the level of the latter with theoretical uncertainties taken into account is not significant in the scan. We find the values of the CP-observables $\langle a_{\text{CP}}^{(1,3)} \rangle$ to be within -0.2 and +0.2, while $\langle a_{\text{CP}}^{(2)} \rangle$ is unconstrained by current data. To illustrate the impact of a future measurement of the CP asymmetry, we add hypothetical data with a reduced experimental uncertainty $\langle a_{\text{CP}}^{(1)} \rangle = 0.074 \pm 0.01$ to the scan. The central value is inspired by the BSM benchmark, see Table I. As can be seen from Fig. 3, the extended data set (solid, black lines) adds complementary constraints on the phases, which become challenging to the SM (green square).

IV. SUMMARY

Building on previous works on CP symmetries [14] we identified CP asymmetries $a_{\text{CP}}^{(i)}$, $i = 1, 2, 3$ and $a_{\text{CP}}^{\text{mix}}$ with no leading form factor dependence from the angular distribution of $\bar{B} \rightarrow \bar{K}^*(\rightarrow \bar{K}\pi)l^+l^-$ and of $\bar{B}_s, B_s \rightarrow \phi(\rightarrow K^+K^-)l^+l^-$ decays at low hadronic recoil. The simple amplitude structure following from the heavy quark framework of Ref. [10] in this kinematical region has been crucial in doing so. We find that the largest uncertainty in these CP asymmetries stems from the renormalisation scale dependence at NLO in α_s , which is sizeable, followed by subleading $1/m_b$ corrections, see Section II B.

Being strongly parametrically suppressed in the SM, the CP asymmetries are nulltests of the SM. At the same time the available experimental constraints allow for large BSM effects in the (low recoil q^2 -integrated) asymmetries $\langle a_{\text{CP}}^{(1,3)} \rangle$ up to ~ 0.2 . The asymmetry $\langle a_{\text{CP}}^{(2)} \rangle$ is due to its possibly vanishing normalisation presently unconstrained. The mixing asymmetry in $\bar{B}_s, B_s \rightarrow \phi(\rightarrow K^+K^-)l^+l^-$, $\langle a_{\text{CP}}^{\text{mix}} \rangle$ exhibits for realistic values of the mixing parameters little sensitivity to the latter and is numerically close to $\langle a_{\text{CP}}^{(3)} \rangle$. Note that both $a_{\text{CP}}^{\text{mix}}$ and $a_{\text{CP}}^{(3)}$ do not require flavour tagging.

By testing the effective theory Eq. (2.1) against the existing data of $b \rightarrow s\gamma$ and $b \rightarrow sl^+l^-$ decays in the presence of BSM CP violation, we extract the allowed ranges of the Wilson coefficients $\mathcal{C}_{9,10}$ shown in Figs. 2 and 3. We find consistency with a related recent analysis for real-valued coefficients [14] and with the SM. Parameter points with order one deviations from the SM are presently allowed.

To maximize the exploitation of data we strongly suggest to provide the future CP symmetries and asymmetries in q^2 -bins accessible to systematic theory calculations, such as $1\text{--}6\text{ GeV}^2$ and $\geq 14\text{ GeV}^2$, similar to the common binning used in both recent Belle and CDF analyses [31, 32]. For completeness we give here the low recoil SM predictions for the basic CP-averaged observables, the branching ratio, the forward-backward asymmetry and the fraction of longitudinally polarised K^* mesons,

$$10^7 \times \int_{14\text{ GeV}^2}^{(m_B - m_{K^*})^2} dq^2 \frac{d\mathcal{B}_{\text{SM}}}{dq^2} = 2.86 \left. \begin{array}{c} +0.87 \\ -0.74 \end{array} \right|_{\text{FF}} \left. \begin{array}{c} +0.11 \\ -0.10 \end{array} \right|_{\text{SL}} \left. \begin{array}{c} +0.10 \\ -0.19 \end{array} \right|_{\text{CKM}} \left. \begin{array}{c} +0.08 \\ -0.04 \end{array} \right|_{\text{SD}}, \quad (4.1)$$

$$\langle A_{\text{FB}} \rangle_{\text{SM}} = -0.41 \pm 0.07 \left. \begin{array}{c} \pm 0.007 \\ \pm 0.007 \end{array} \right|_{\text{FF}} \left. \begin{array}{c} +0.002 \\ -0.003 \end{array} \right|_{\text{SL}} \left. \begin{array}{c} \pm 0.007 \\ \pm 0.007 \end{array} \right|_{\text{SD}}, \quad (4.2)$$

$$\langle F_{\text{L}} \rangle_{\text{SM}} = 0.35 \left. \begin{array}{c} +0.04 \\ -0.05 \end{array} \right|_{\text{FF}} \pm 0.003 \left. \begin{array}{c} \pm 0.003 \\ \pm 0.003 \end{array} \right|_{\text{SL}}, \quad (4.3)$$

respectively. The predictions are based on the improved uncertainty estimate for the subleading power corrections of Appendix A and updated CKM input from [15], but follow [14] otherwise. The largest uncertainty in the above observables stems from the form factors (FF). Uncertainties smaller than a permille are not given explicitly.

We stress that the transversity observables allow for consistency checks of the theoretical low recoil framework. Since the OPE-breaking corrections generically will spoil the transversity amplitude relation Eq. (1.1) on which the predictions *i*) - *iv*) listed in the Introduction are based on, the performance of the employed heavy quark framework can be tested experimentally.

Acknowledgments

We thank Matthew Wingate for useful communication on the lattice results for f_{B_s} and Frederik Beaujean for advice on multidimensional analyses. We are thankful to the technical team of the Φ Do HPC cluster, without which we could not have performed our scans. D.v.D. is grateful to Ciaran McCreesh for valuable advice regarding the numerical implementation. We are grateful to Christian Wacker for uncovering an error in the computation of the confidence regions. This work is supported in part by the Bundesministerium für Bildung und Forschung (BMBF).

Appendix A: Estimate of the subleading power corrections

The subleading power corrections to $\bar{B} \rightarrow \bar{K}^* l^+ l^-$ decays at low recoil arise from the form factor (Isgur-Wise) relations beyond the heavy quark limit and the contributions of subleading opera-

tors to the OPE [10]. Both contributions involve the same (three) HQET form factors, which are essentially unknown (see [12] for model estimates) but in principle are accessible to lattice calculations.

The subleading corrections to the form factor relations enter the decay amplitudes multiplying the small coefficient \mathcal{C}_7 . The subleading OPE-corrections involve presently unknown Wilson coefficients of order α_s . Their knowledge would require a generalisation of the 2-loop calculation of [33] for off-shell quark states. The latter gives in general complex-valued results, introducing new strong phases. Both corrections can therefore be parameterised as

$$\tilde{r}_i \sim \pm \frac{\Lambda_{\text{QCD}}}{m_b} \left(\mathcal{C}_7 + \alpha_s(\mu) e^{i\delta_i} \right), \quad i = a, b, c. \quad (\text{A1})$$

The exact form of the \tilde{r}_i can be inferred from $\tilde{r}_i = r_i \mathcal{C}_9^{\text{eff}}$, with the r_i given in Ref. [10]. As already noted, the strong phases δ_i are currently not known.

The transversity amplitudes depend on the \tilde{r}_i as follows, see [14] for details,

$$A_{\perp}^{L,R} = +i \left[(\mathcal{C}_9^{\text{eff}} \mp \mathcal{C}_{10}) + \kappa \frac{2\hat{m}_b}{\hat{s}} \mathcal{C}_7^{\text{eff}} + \tilde{r}_a \right] f_{\perp}, \quad (\text{A2})$$

$$A_{\parallel}^{L,R} = -i \left[(\mathcal{C}_9^{\text{eff}} \mp \mathcal{C}_{10}) + \kappa \frac{2\hat{m}_b}{\hat{s}} \mathcal{C}_7^{\text{eff}} + \tilde{r}_b \right] f_{\parallel}, \quad (\text{A3})$$

$$A_0^{L,R} = -i \left[(\mathcal{C}_9^{\text{eff}} \mp \mathcal{C}_{10}) + \kappa \frac{2\hat{m}_b}{\hat{s}} \mathcal{C}_7^{\text{eff}} \right] f_0 - i N m_B \frac{(1 - \hat{s} - \hat{m}_{K^*}^2)(1 + \hat{m}_{K^*})^2 \tilde{r}_b A_1 - \hat{\lambda} \tilde{r}_c A_2}{2 \hat{m}_{K^*} (1 + \hat{m}_{K^*}) \sqrt{\hat{s}}}, \quad (\text{A4})$$

which mildly breaks the universality of Eq. (1.1). In the numerical implementation we vary the \tilde{r}_i and δ_i for $i = a, b, c$ independently within $|\tilde{r}_i| \leq 0.1$ and $\delta_i \in [-\pi/2, +\pi/2]$ and allow for both signs in Eq. (A1). The resulting uncertainty is termed (SL) in this work. The SM predictions of some basic CP-conserving observables are given in Section IV. Note that this estimation improves on our previous works [14], where we introduced for each of the transversity amplitudes one real scaling factor for the corrections to the form factor relations and additionally for each left- and right-handed amplitude six real scaling factors in order to estimate the subleading OPE-corrections.

-
- [1] F. Kruger, L. M. Sehgal, N. Sinha and R. Sinha, Phys. Rev. D **61**, 114028 (2000) [Erratum-ibid. D **63**, 019901 (2001)], [arXiv:hep-ph/9907386].
- [2] M. Beneke, T. Feldmann, D. Seidel, Nucl. Phys. **B612**, 25-58 (2001), [hep-ph/0106067].
- [3] M. Beneke, T. Feldmann, D. Seidel, Eur. Phys. J. **C41**, 173-188 (2005), [hep-ph/0412400].
- [4] C. Bobeth, G. Hiller and G. Piranishvili, JHEP **0807**, 106 (2008), [arXiv:0805.2525 [hep-ph]].

- [5] U. Egede *et al.*, JHEP **0811**, 032 (2008), [arXiv:0807.2589 [hep-ph]].
- [6] W. Altmannshofer *et al.*, JHEP **0901**, 019 (2009), [arXiv:0811.1214 [hep-ph]].
- [7] C. Bobeth, G. Hiller and G. Piranishvili, arXiv:0911.4054 [hep-ph].
- [8] U. Egede, T. Hurth, J. Matias *et al.*, JHEP **1010**, 056 (2010), [arXiv:1005.0571 [hep-ph]].
- [9] A. Khodjamirian, T. Mannel, A.A. Pivovarov and Y.M. Wang, JHEP **1009** (2010) 089, [arXiv:1006.4945 [hep-ph]].
- [10] B. Grinstein and D. Pirjol, Phys. Rev. D **70**, 114005 (2004), [arXiv:hep-ph/0404250].
- [11] M. Beylich, G. Buchalla and T. Feldmann, arXiv:1101.5118 [hep-ph].
- [12] B. Grinstein and D. Pirjol, Phys. Lett. B **533**, 8 (2002), [arXiv:hep-ph/0201298].
- [13] J. L. Hewett *et al.*, arXiv:hep-ph/0503261.
- [14] C. Bobeth, G. Hiller and D. van Dyk, JHEP **1007**, 098 (2010), [arXiv:1006.5013 [hep-ph]].
- [15] J. Charles *et al.* [CKMfitter Group Collaboration], Eur. Phys. J. **C41**, 1-131 (2005), [hep-ph/0406184].
We use the numerical results as presented at ICHEP2010, Paris, France, July 22-28, 2010.
- [16] F. Kruger and L. M. Sehgal, Phys. Lett. B **380**, 199 (1996), [arXiv:hep-ph/9603237].
- [17] K. Nakamura *et al.* [Particle Data Group], J. Phys. G **37**, 075021 (2010).
- [18] A. Ali, P. Ball, L. T. Handoko and G. Hiller, Phys. Rev. D **61**, 074024 (2000), [arXiv:hep-ph/9910221].
- [19] G. Buchalla, G. Hiller and G. Isidori, Phys. Rev. D **63**, 014015 (2000), [arXiv:hep-ph/0006136].
- [20] F. Kruger and E. Lunghi, Phys. Rev. D **63**, 014013 (2001), [arXiv:hep-ph/0008210].
- [21] A. K. Alok, A. Datta, A. Dighe, M. Duraisamy, D. Ghosh and D. London, arXiv:1103.5344 [hep-ph].
- [22] R. Fleischer and I. Dunietz, Phys. Rev. D **55**, 259 (1997), [arXiv:hep-ph/9605220].
- [23] E. Barberio *et al.* [Heavy Flavor Averaging Group], arXiv:0808.1297 [hep-ex].
Online <http://www.slac.stanford.edu/xorg/hfag> from March 2010.
- [24] M. Misiak *et al.*, Phys. Rev. Lett. **98**, 022002 (2007), [arXiv:hep-ph/0609232].
- [25] T. Becher and M. Neubert, Phys. Rev. Lett. **98**, 022003 (2007), [arXiv:hep-ph/0610067].
- [26] D. van Dyk *et al.*, Online <http://project.het.physik.tu-dortmund.de/source/eos/tag/lowrecoil-cp>.
- [27] E. Gamiz, C. T. H. Davies, G. P. Lepage, J. Shigemitsu and M. Wingate [HPQCD Collaboration], Phys. Rev. D **80** (2009) 014503, [arXiv:0902.1815 [hep-lat]].
- [28] J. Simone *et al.* [Fermilab Lattice and MILC Collaborations], PoS **LATTICE2010** (2010) 317.
- [29] M. Palutan on behalf of the LHCb Collaboration at BEAUTY 2011, 13th International Conference on B-Physics at Hadron Machines, April 4th-8th 2011, Amsterdam, The Netherlands.
- [30] B. Aubert *et al.* [BABAR Collaboration], Phys. Rev. Lett. **102**, 091803 (2009), [arXiv:0807.4119 [hep-ex]].
- [31] J. T. Wei *et al.* [BELLE Collaboration], Phys. Rev. Lett. **103**, 171801 (2009), [arXiv:0904.0770 [hep-ex]].
- [32] T. Aaltonen *et al.* [CDF Collaboration], arXiv:1101.1028 [hep-ex].
- [33] D. Seidel, Phys. Rev. D **70** (2004) 094038, [arXiv:hep-ph/0403185].